described in ref 20. Capillary GC was performed by using a Varian 3300 GC with a Varian 4290 integrator and a Quadrex 50M 007 Carbowax 20M column No. 507011. ^{19}F NMR spectra were recorded on a Bruker WM490 (460MHz) spectrometer with trifluoroacetic acid as an external reference.

Asymmetric Epoxidation. Asymmetric epoxidations were carried out in CH_2Cl_2 at −25 °C following the detailed procedure of Sharpless,[1c,12b,c] with the exception that 4 Å MS were added to reactions of **2** and **6**. Epoxidation of 1,4-pentadien-3-ol: workup with ether, saturated sodium sulfate. Careful solvent removal and flash chromatography (1/1 ether/pentane) provided the monoepoxy alcohol contaminated with DIPT. Epoxidation of 1,7-dibenzyloxy-2(*E*),5(*E*)-heptadien-4-ol: workup with 10% aqueous tartaric acid, NaOH hydrolysis. Flash chromatography (1/2 ether/petroleum ether) provided the pure monoepoxy alcohol. Epoxidation of 2,4-dimethyl-1,4-pentadien-3-ol: workup with ether, saturated sodium sulfate. Flash chromatography (1/3 ether/petroleum ether) provided the pure monoepoxy alcohol.

MTPA Esters. MTPA esters were prepared in CCl_4/pyridine as described in ref 20 or in CH_2Cl_2 with triethylamine and (dimethylamino)pyridine and were purified by filtration with SiO_2.

Product Analysis. Diastereomeric excess was determined by comparison of the capillary GC trace of the reaction mixture to that of mixtures of diasteromers prepared via alternative procedures or via similar analysis with ^{19}F NMR of the *S*-MTPA esters. Enantiomeric excess in Tables II and III was determined by ^{19}F NMR analysis (detection limit ca. 97% ee) of the *S*-MTPA ester derivatives of the epoxidation products obtained from the reaction of the achiral substrates with the Sharpless reagents derived from (+)- and (−)-DIPT. Subsequent to these studies, the derivatizing agent *S*-MTPA acid chloride was determined to exist in 97% ee (vide supra). The data in these tables are uncorrected. The enantiomeric excess in Table IV was determined by capillary GC analysis of the *S*-MTPA esters of the epoxidation products. We were able to detect a 300:1 mixture, with base line separation, of the Mosher esters **11** and **10**, thereby establishing a detection limit of >99.3% ee. The entry in Table IV with >99.3% ee signifies that we were not able to detect the minor isomer. In these studies, *S*-MTPA acid chloride was employed that was derived from *S*-MTPA acid that had been triply recrystallized as its (−)-α-phenethylamine salt.

Acknowledgment. This research has been supported by the NIH (GM-30738), NSF (Presidental Young Investigator Award), and Pfizer, Inc., to whom we are grateful. We thank Professors K. Barry Sharpless and H. B. Kagan for generous exchanges of information.

Registry No. **2**, 922-65-6; **3**, 102490-00-6; **4**, 100017-22-9; **6**, 106319-54-4; **7**, 106319-55-5; **8**, 106400-06-0; **9**, 38614-40-3; **10**, 106400-07-1; **11**, 106319-56-6.

Supplementary Material Available: Details of the derivation of eq 1 (12 pages). Ordering information is given on any current masthead page.

Reactions of Crystalline (*R*)-(−)- and (*S*)-(+)-Mandelic Acid with Amines. Crystal Structure and Dipole Moment of (*S*)-Mandelic Acid. A Method of Determining Absolute Configuration of Chiral Crystals

A. O. Patil, W. T. Pennington, I. C. Paul,* D. Y. Curtin,* and C. E. Dykstra

Contribution from the Department of Chemistry, University of Illinois, Urbana, Illinois 61801.
Received August 5, 1986

Abstract: The reaction of (+)-1-phenylethylamine vapor occurs more rapidly with single crystals of (+)-mandelic acid to form the (+)(+) or "p" salt than with (−)-mandelic acid to give the (+)(−) or "n" salt, known to be the less soluble on crystallization from solution. The reaction fails to show the anisotropy characteristic of some other reactions of crystalline acids with chiral gases. The crystal structure of (*S*)-(+)-mandelic acid has been determined. The structure is monoclinic, $P2_1$, with a = 8.629 (1) Å, b = 5.861 (1) Å, c = 15.185 (2) Å, β = 102.76 (1)°, and Z = 4. The structure was determined by direct methods and refined to R = 0.035 for the 1347 reflections recorded with a single-crystal diffractometer. The dipole moments of the mandelic acid molecules in the conformations found in the crystal structure determination were calculated by an ab initio SCF method. These results, together with the crystal morphology and known absolute configuration of the crystals, can be used to determine the direction of the electric dipole of single crystals of (*S*)-mandelic acid. The result is in agreement with the direction determined by spraying heated crystals with the powder mixture of Burker in the classic test for absence of a crystal center of symmetry. When the argument is inverted it provides a method for determining the absolute configuration of chiral, electrically polar molecules from the X-ray crystal structure, crystal morphology, and direction of the electric dipole of the crystal. The reaction of mandelic acid crystals with phenylethylamine vapor is discussed in terms of the crystal structure. A survey has been made of the solid–gas reactions of mandelic acid with ammonia, 2-butylamine, and *tert*-butylamine.

It has been shown[1] that a chiral gas, (*R*)-(+)- or (*S*)-(−)-1-phenylethylamine (**1**), in its reaction with single crystals of chiral acids such as (*R*)-(−)- and (*S*)-(+)-mandelic acid [(*R*)- and (*S*)-**2**)] shows a preference for one enantiomeric crystal over the other. Thus amine (*R*)-(+)-**1** reacted more rapidly with (*S*)-(+)-acid **2** than with its enantiomer. No further investigation of this reaction was made at that time. Because of our interest[2] in polar crystals, the enantiomers of mandelic acid were noteworthy since they have been known[3,4] for many years to crystallize in the polar point group 2, space group $P2_1$.

More recently the pyroelectric effect has been found useful in determining the direction of the electric dipole induced by heating

(*R*)-(+)-**1** (*S*)-(+)-**2**

(1) Lin, C.-T.; Curtin, D. Y.; Paul, I. C. *J. Am. Chem. Soc.* **1974**, *96*, 6199–6200.

(2) (a) Paul, I. C.; Curtin, D. Y. *Science* **1975**, *187*, 19–26. (b) Curtin, D. Y.; Paul, I. C. *Chem. Rev.* **1981**, *81*, 526–541. (c) Duesler, E. N.; Kress, R. B.; Lin, C.-T.; Shiau, W.-T.; Paul, I. C.; Curtin, D. Y. *J. Am. Chem. Soc.* **1981**, *103*, 875–879. (d) Chaing, C. C.; Lin, C.-T.; Wang, A. H.-J.; Curtin, D. Y.; Paul, I. C. *J. Am. Chem. Soc.* **1977**, *99*, 6303–6309.

(3) See: Groth, P. *Chemische Kristallographie*; Verlag von Wilhelm Engelmann: Leipzig, 1917; Vol. 4, p 559. Traube, H. *Chem. Ber.* **1859**, *32*, 2385.

(4) Furberg, S. *Res. London*, **1951**, *4*, 192–193; *Struct. Rep.* **1951**, *15*, 463–464.

0002-7863/87/1509-1529$01.50/0

crystals of *p*-bromobenzoic anhydride, and it was pointed out that there is a relationship between the direction of the polar axis of a chiral crystal and the absolute configuration of the molecules in the crystal.[5]

It was of interest, therefore, to investigate in more detail the behavior of enantiomers of mandelic acid in their reactions with chiral gases and to attempt to correlate the reactivity with the internal structure of the crystal.

The structure of the racemic form of mandelic acid has been reported.[6] This paper reports the X-ray crystal struture determination[7,8] of (*S*)-(+)-mandelic acid, (*S*)-(+)-**2**, and the behavior of the mandelic acid isomers in their reactions with gases.

In the course of this work a knowledge of the direction of the electric dipole of a crystal of (*R*)- or (*S*)-mandelic acid was needed so we report on the use of the ab initio calculations for this purpose.

We discuss also the relationship among the absolute configuration of molecules, the direction of the dipole moment, and crystal morphology for mandelic acid.

Experimental Section

Microanalyses were carried out by J. Nemeth and his associates. Fourier transform infrared spectra were obtained in Nujol mull with a Nicolet 7000 FTIR spectrophotometer or an IBM IR/32 FTIR spectrophotometer. Differential scanning calorimetry scans were recorded with a DuPont 900 Thermal Analyzer. DSC temperatures reported are extrapolated onset values. X-ray powder photographs (Ni-filtered Cu Kα radiation) were made with a Debye–Scherrer powder camera. Optical goniometric data were measured on a Tecom two-circle optical goniometer. Photographs were taken with a Beseler Topcon Super D camera mounted on a Bausch and Lomb Model LS dynoptic polarizing microscope with use of 160 ASA Ektachrome film.

(*R*)-(−)- and (*S*)-(+)-mandelic acid (99%+) were obtained from the Aldrich Chemical Co. Either enantiomer gave "hexagonal"- and "tetragonal"-shaped plates when crystallized from chloroform or from ethanol–methylene chloride (9:1). One of the "hexagonal" plates was employed for the crystal structure determination described below. Either enantiomer, when sublimed at 110–112 °C (atmospheric pressure) with no cooling of the cold finger, gave very thin needles. X-ray powder photographs of the needles were identical with photographs of the other two crystal habits. Differential scanning calorimetry of the (+) enantiomer showed a single sharp melting endotherm at 136 °C. DSC scans of control mixtures showed that less than 0.7% of racemic **2** would have been detected if present.

Sources and Purity of the Amines. (*S*)-(−)- and (*R*)-(+)-Phenylethylamine (**1**) (>98% optical purity) were purchased from the Aldrich Chemical Co. The commercial samples were found by a chromatographic method[9] to contain not more than 1.5% of the opposite enantiomer. (±)-2-Butylamine and *tert*-butylamine were obtained from Eastman Kodak Co.

X-ray Structure Analysis of (*S*)-(+)-Mandelic Acid. A "hexagonal" crystal described above was employed for the X-ray structure determination.

Crystal Data: $C_8H_8O_3$, Mw = 152.2, monoclinic, a = 8.629 (1) Å, b = 5.861 (1) Å, c = 15.185 (2) Å, β = 102.76 (1)°, V = 749 × 10^{-24} cm^3, Z = 4, D_{calcd} = 1.349 g/cm^3, space group, $P2_1$.

Unit cell parameters were determined by a least-squares fit of the setting angles for 15 carefully centered high-order reflections (66° < 2θ < 94°). A total of 1595 unique measurements (R_{merge} = 0.023), made on a Syntex $P2_1$ diffractometer employing graphite monochromated Cu Kα radiation (λ = 1.54178 Å), resulted in 1347 reflections with intensities greater than 3$\sigma(I)$. Scans were made in the $\theta/2\theta$ mode at speeds ranging from 2.02 to 19.53 deg/min for one quartet of data ($h\,\bar{k}\pm l$) out to a 2θ value of 143°.

Table I. Final Atomic Coordinates for (*S*)-Mandelic Acid

	x/a	*y/b*	*z/c*
O1A	0.6835 (3)	0.9434 (5)	0.3634 (1)
O2A	0.5379 (2)	0.7771 (5)	0.4496 (1)
O3A	0.6152 (3)	0.3601 (4)	0.4071 (1)
C1A	0.6235 (2)	0.7692 (5)	0.3973 (1)
C2A	0.6768 (3)	0.5416[a]	0.3643 (1)
C3A	0.6259 (2)	0.5211 (5)	0.2623 (1)
C4A	0.7232 (3)	0.6018 (7)	0.2081 (1)
C5A	0.6750 (4)	0.5863 (8)	0.1142 (2)
C6A	0.5328 (4)	0.4898 (6)	0.0742 (2)
C7A	0.4381 (3)	0.4082 (8)	0.1277 (2)
C8A	0.4805 (3)	0.4249 (7)	0.2215 (2)
O1B	0.8150 (3)	0.9363 (5)	0.6367 (1)
O2B	0.9607 (2)	0.7729 (5)	0.5501 (1)
O3B	0.9030 (2)	0.3523 (4)	0.6016 (1)
C1B	0.8779 (2)	0.7625 (5)	0.6039 (1)
C2B	0.8317 (3)	0.5354 (4)	0.6397 (1)
C3B	0.8821 (2)	0.5221 (5)	0.7419 (1)
C4B	0.7816 (3)	0.4229 (7)	0.7907 (1)
C5B	0.8295 (3)	0.4033 (8)	0.8840 (2)
C6B	0.9746 (4)	0.4825 (6)	0.9290 (2)
C7B	1.0740 (3)	0.5797 (8)	0.8811 (2)
C8B	1.0283 (3)	0.5989 (7)	0.7881 (1)
H1A	0.654 (3)	1.054 (4)	0.381 (2)
H2A	0.796 (3)	0.547 (4)	0.383 (2)
H3A	0.566 (3)	0.408 (4)	0.440 (2)
H4A	0.818 (2)	0.665 (4)	0.237 (2)
H5A	0.742 (3)	0.630 (4)	0.077 (2)
H6A	0.508 (3)	0.486 (4)	0.009 (2)
H7A	0.345 (3)	0.333 (4)	0.101 (2)
H8A	0.416 (3)	0.372 (4)	0.259 (1)
H1B	0.843 (3)	1.057 (4)	0.615 (2)
H2B	0.709 (3)	0.528 (4)	0.626 (2)
H3B	0.941 (3)	0.393 (4)	0.561 (2)
H4B	0.672 (3)	0.370 (4)	0.759 (1)
H5B	0.758 (2)	0.342 (4)	0.921 (1)
H6B	1.013 (3)	0.472 (4)	0.989 (2)
H7B	1.164 (3)	0.616 (4)	0.910 (2)
H8B	1.099 (3)	0.653 (4)	0.756 (2)

[a] Fixed to determine the origin.

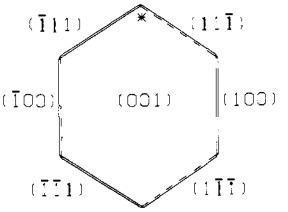

Figure 1. Sketch of a crystal of (*R*)-(−)- or (*S*)-(+)-mandelic acid. Note that the major face is (001). The polar *b* axis is in the plane of the page pointing toward the top of the page. The *a* axis is to the right in the page with the (100) faces tilted toward the viewer. The end of (*R*)-(−) crystal marked with a "*" becomes coated with the blue (lycopodium) powder and the other end red-orange. An (*S*)-(+) crystal shows the colors reversed in the pyroelectric test.

Periodic measurement of three standard reflections indicated a 5.7% decline in intensity over the 35 h of X-ray exposure time; a linear correction factor was applied to compensate for this decomposition. Data were corrected for Lorentz and polarization effects, and an analytical absorption correction ($\mu_{CuK\alpha}$ = 8.32 cm^{-1}) was applied which resulted in transmission factors ranging from 0.72 to 0.86.

The structure solution, accomplished with use of direct methods (MULTAN80),[10] proved rather difficult due to the pseudocentering operation which related the two molecules (hereafter referred to as A and B) in the crystal asymmetric unit. The automatic scaling of parity classes performed by MULTAN80 resulted in extremely high E values for the systematically weak reflections (hkl, $h + k$ odd). Individual scaling was required to yield an E map which revealed the positions of 16 of the 22 non-hydrogen atoms. The positions of all remaining atoms, including the

(5) Patil, A. A.; Curtin, D. Y.; Paul, I. C. *J. Am. Chem. Soc.* **1985**, *107*, 726–727.

(6) (a) Wei, K.-T.; Ward, D. L. *Acta Crystallogr.* **1977**, *B33*, 797–800. (b) Cameron, T. S.; Duffin, M. *Crysta. Struct. Commun.* **1974**, *3*, 539–541. (c) Rose, H. A. *Anal. Chem.* **1952**, *24*, 1680–1681.

(7) After the structure determination described in this paper was completed we became aware of a statement (ref 8, p 25) that the structure had been previously determined with a reference to T. C. Van Soest, unpublished results, and a Thesis by M. Cesario, Orsay, 1976. This structure determination has never been included in the Cambridge File, however.

(8) Jacques, J.; Collet, A.; Wilen, S. H. *Enantiomers, Racemates, and Resolution*; Wiley: New York, 1981.

(9) We are indebted to Matthew Grannen and Professor W. H. Pirkle of this department for these results.

(10) Main, P.; Fiske, S. J; Hull, S. E.; Lessinger, L.; Germain, G.; Declercq, J. P.; Woolfson, M. M. MULTAN80—a system of computer programs for the automatic solution of crystal structures from X-ray data, University of York, England, and University of Louvain, Belgium, 1980.

hydrogen atoms, were determined by conventional least-squares and difference Fourier techniques.

Full-matrix least-squares refinement was based on 1347 non-zero reflections and 248 parameters, including positional and anisotropic thermal parameters for the non-hydrogen atoms and positional parameters and a group thermal parameter for the hydrogen atoms. No parameter shifted by more than 0.05σ in the final cycle which produced values of $R = 0.035$ $R_w = 0.060$, and GOF = 1.29. The weighting scheme, $w = [4.04/(\sigma^2(F) + 0.002\ F^2)]$, showed no dependence on the magnitude of F or on the value of $\sin\theta$. A final difference Fourier map was featureless, with maximum and minimum peaks corresponding to 0.17 and -0.12 $e^-/Å^3$, respectively. The atomic scattering factors for the neutral atoms were those of Cromer and Waber.[11] All computations, other than structure solution, were performed with the SHELX76 package of computer programs.[12] Atomic coordinates are given in Table I. A list of observed and calculated structure factors and a table of anisotropic thermal parameters have been deposited.

Crystal Morphology of (*S*)-(+)-Mandelic Acid. The major faces of the "hexagonal" plates and the long crystal direction of (*S*)-(+)-**2** were shown by orientation with the X-ray diffractometer to be {001} and [010]. Optical goniometry was used to establish the side faces as {100} and the end faces as $\{11\bar{1}\}$ and $\{1\bar{1}\bar{1}\}$ (see Figure 1). These assignments are in agreement with those made by Traube,[3] who, however, found also {110} and $\{1\bar{1}0\}$.

The needles obtained by sublimation were shown by alignment on an X-ray diffractometer to be oriented along [010] but the faces were not sufficiently well developed to permit their identification. X-ray powder photographs of the "hexagonal" crystals from ethanol–methylene chloride showed the same d-spacings as those of the needles from sublimation.

The "tetragonal" crystals were found to have interfacial angles corresponding to the end faces of the "hexagonal" crystals but with the side {100} faces missing.

The direction of the twofold crystal axis of the "hexagonal" crystals of (*S*)-(+)-**2** was confirmed by etching of single crystals by suspending them for 5 min in cyclohexane. Triangular etch pits on the (001) face pointed toward (100), and, on the opposite side $(00\bar{1})$, in the opposite direction. Similar behavior was observed with (*R*)-(−)-**2**, but racemic mandelic acid gave no etch pits under these conditions.

Reactions of Crystalline Mandelic Acid 2 with Gases. Single crystals of **2** were placed in a small compartment made by cementing two microscope slides to a metal ring with entrance and exit tubes for introducing a gas as described previously.[2c]

(a) **Reaction of (*S*)-(+)-2 with Ammonia.** When single crystals of (*S*)-(+)-**2** in the apparatus above were exposed to ammonia gas the crystals were found to begin to melt in approximately 5 min even when the ammonia was introduced at a very slow rate (10 bubbles/min). Melting was complete in 2 h. The liquid solidified on standing to give microcrystalline salt which showed extinction between crossed polarizing filters.

(b) Reaction of (*S*)-(+)-2 with (±)-2-Butylamine. Single crystals of (+)-**2** were placed in a reaction cell, and a drop of (±)-2-butylamine was inserted through the entrance port with a syringe. Microscopic examination showed that reaction began immediately at the side faces while the (001) face remained clear. A reaction front moved from the sides toward the center of the major face of the crystal, and the crystal became completely opaque in about 1 min. No expansion of the crystal along the *a* and *b* axes (as viewed onto the (001) face) was evident. When viewed from the side, marked expansion along the (001) direction was evident.

When a few crystals (13.4 mg) were allowed to react for 24 h and then placed in a vacuum desiccator to remove excess amine and reweighed, the weight gain was 6.5 mg (theoretical for 100% reaction 6.4 mg).

Calcd for $C_{23}H_{19}NO_3$: C, 64.0; H, 8.5; N, 6.2. Found: C, 63.8; H, 8.4; N, 6.2.

When a fully reacted crystal was mounted on a precession camera no diffraction spots suggestive of a single crystalline product were observed.

(c) Reaction of (*S*)-(+)-2 with *tert*-Butylamine. When a "hexagonal" crystal of (*S*)-(+)-**2** in a cell as described above was exposed to the vapor from a drop of *tert*-butylamine the entire crystal appeared to develop a dull appearance almost immediately but continued to show good extinction between crossed polarizing filters. After 2 h the end faces, $(11\bar{1})$, $(\bar{1}11)$, $(\bar{1}\bar{1}1)$, and $(1\bar{1}\bar{1})$, showed clear evidence of preferential reaction compared to the {100} faces. After 4 h a reaction front had moved from all sides toward the center of the crystal which still showed extinction, but the top surface too became coated with reaction product eventually. Observation of a number of crystals suggested that in early stages of the reaction the two faces at one end of the polar [010] axis reacted more rapidly than those at the other though the preference was slight.

(d) Reaction of (*S*)-(+)-2 with (*R*)-(+)-1-Phenylethylamine (1). A sample tube open at one end containing a few single crystals (10.6 mg) of (*S*)-(+)-**2** was placed in a larger sample tube containing 0.5 mL of (*R*)-(+)-**1**, and the outer tube was sealed, care being taken that no liquid amine came into direct contact with the crystals. After 24 h the sample was subjected to vacuum for 1 h to remove the excess amine and weighed. The increase in weight suggested that 50% reaction had occurred. A combustion analysis was obtained.

Anal. Calcd for 52% reaction: C, 67.9; H, 6.3; N, 3.5. Found: C, 67.9; H, 6.4; N, 3.4.

This partially reacted crystal mounted on a precession camera showed strong diffraction characteristics of unreacted (*S*)-(+)-**2**. X-ray photographs with a Weissenberg camera showed in addition powder lines attributed to microcrystalline (+)(+) salt. The remaining sample was allowed to react further for 9 days after which the elemental analysis was that to be expected for the 1:1 salt.

Anal. Calcd for the 1:1 salt: C, 70.3; H, 7.1; N, 5.1. Found: C, 70.3; H, 7.0; N, 5.1.

Examination of the reacted crystal at this stage showed no diffraction corresponding to unreacted acid and a powder photograph was identical with a photograph of the (*S*)-(+)-acid (*R*)-(+)-amine salt prepared by crystallization from solution. In another experiment qualitatively similar results were obtained but the weight gain after 4 days corresponded to 78% reaction.

Since viewed looking onto (001) a crystal of (*S*)-(+)-**2** showed, during the reaction with (*R*)-(+)-**1**, no appreciable increase in area, and because this reaction requires a substantial increase in volume, a "hexagonal" crystal of (*S*)-(+)-**2** was mounted in a capillary tube and attached to the wall of the reaction cell in such a way that any expansion along the *c* direction could be observed microscopically. Two drops of (*R*)-(+)-amine **1** were inserted into the cell, and the thickness of the crystal was compared with a 2-mm scale with marks 0.01 mm apart. The crystal which was initially 0.12-mm thick after 6 days had expanded to 0.225 mm, or almost twice the original thickness. A similar change was observed in a duplicate experiment. Similar expansion along the *c* axis rather than *a* and *b* was found in the reaction of (*S*)-(+)-**2** with (±)-2-butylamine.

(e) Competition of (*S*)-(+)-2 and (*R*)-(−)-2 for (*S*)-(−)-1. Two needles each of (*S*)-(+)- and (*R*)-(−)-**2** were observed with a microscope when two drops of (*S*)-**1** were placed near them. The crystal of (*R*)-(−) acid showed signs of extensive change after 9 min and had become completely opaque in 6 h while the (*S*)-(+) acid showed very little indication of reaction in that time and required 24 h to become completely opaque. "Hexagonal" crystals of the enantiomers of acid **2** behaved similarly. A competition of needles of (*S*)-(+)- and (*R*)-(−)-**2** for (*R*)-(+)-amine gave comparable results (with the opposite preference, as expected).

Determination of the Direction of the Polar Axis of "Hexagonal" Crystals of Acid 2 by the Pyroelectric Effect. A crystal of (*S*)-(+)-**2** was heated on a glass slide in an oven at 80 °C for 0.5 h and then allowed to cool to room temperature. The crystal was sprayed with a stream of a mixture of finely ground lycopodium powder, sulfur, and carmine following the procedure in ref 5. One end of the crystal attracted the red (carmine–sulfur) powder and the other end the blue lycopodium powder. When the crystal is oriented as shown in Figure 1 with the (100) face tilted upward at the right, the red-yellow end of the crystal is toward the top of the page. A similar experiment with a "hexagonal" plate of (*R*)-(−)-**2** in the same orientation as above showed the red-yellow powder at the end of the crystal directed toward the bottom of the page as indicated in Figure 1. "Tetragonal" crystals of **2** also showed good separation of the differently colored powders, but because the {100} faces were missing, the differentiation between (*R*) and (*S*) crystals was not evident from the crystal morphology.

(±)-Mandelic acid (Sigma Chemical Co.) gave "hexagonal" crystals when recrystallized from water, ether, ethanol–methylene chloride (1:1), or chloroform. Solid–gas reactions with (*R*)-(+)-**1**, (+)-2-butylamine, and *tert*-butylamine were similar to the reactions of the enantiomers discussed above; side faces reacted rapidly relative to the top face, but the anisotropy was less pronounced than with the enantiomers.

Results and Discussion

Crystal Structure of (*S*)-(+)-2. In Figure 2 is shown the crystal structure of (*S*)-(+)-**2**. Figure 3 shows a stereoscopic view of one of the two crystallographically independent molecules in the asymmetric unit. Bond lengths and angles are given in Table II.

The dimensions of the two molecules are quite similar within the accuracy of the analysis. In both molecules there is clearly

(11) Cromer, D. T.; Waber, J. T. *International Tables for X-ray Crystallography*; The Kynoch Press: Birmingham, England, 1974; Vol. IV, Table 2.2 B.

(12) Sheldrick, G. M. SHELX76—a program for crystal structure determination, University of Cambridge, England, 1976.

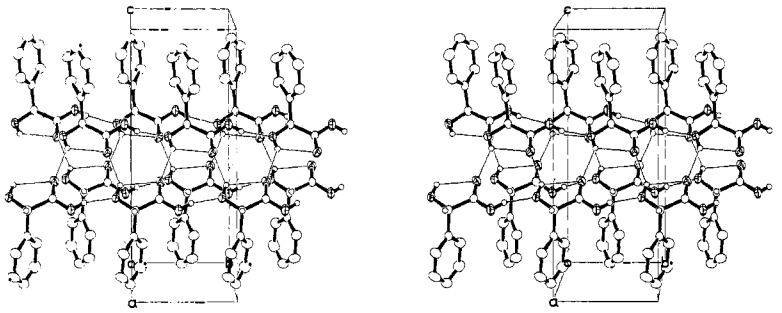

Figure 2. Crystal structure of (*S*)-(+)-mandelic acid showing the two types of hydrogen-bonded chains.

Table II. Intramolecular Distances (Å) and Angles (deg) for (*S*)-Mandelic Acid

molecule A		molecule B	
	Distances		
O1A–C1A	1.301 (4)	O1B–C1B	1.304 (3)
O2A–C1A	1.198 (2)	O2B–C1B	1.199 (2)
O3A–C2A	1.410 (3)	O3B–C2B	1.422 (3)
C1A–C2A	1.532 (3)	C1B–C2B	1.524 (3)
C2A–C3A	1.519 (3)	C2B–C3B	1.518 (3)
C3A–C4A	1.382 (3)	C3B–C4B	1.387 (3)
C4A–C5A	1.397 (3)	C4B–C5B	1.390 (3)
C5A–C6A	1.366 (5)	C5B–C6B	1.368 (5)
C6A–C7A	1.360 (4)	C6B–C7B	1.365 (4)
C3A–C8A	1.390 (3)	C3B–C8B	1.376 (3)
C7A–C8A	1.394 (3)	C7B–C8B	1.385 (3)
O1A–H1A	0.77 (3)	O1B–H1B	0.84 (3)
O3A–H3A	0.78 (3)	O3B–H3B	0.80 (3)
C2A–H2A	1.01 (2)	C2B–H2B	1.03 (2)
C4A–H4A	0.92 (2)	C4B–H4B	1.01 (2)
C5A–H5A	0.93 (2)	C5B–H5B	0.99 (2)
C6A–H6A	0.96 (3)	C6B–H6B	0.90 (3)
C7A–H7A	0.93 (2)	C7B–H7B	0.83 (2)
C8A–H8A	0.93 (2)	C8B–H8B	0.92 (2)
	Angles		
O1A–C1A–O2A	126.1 (3)	O1B–C1B–O2B	125.6 (3)
O1A–C1A–C2A	112.2 (2)	O1B–C1B–C2B	112.4 (2)
O2A–C1A–C2A	121.6 (3)	O2B–C1B–C2B	122.0 (2)
O3A–C2A–C1A	109.5 (2)	O3B–C2B–C1B	110.1 (2)
O3A–C2A–C3A	110.9 (2)	O3B–C2B–C3B	109.0 (2)
C1A–C2A–C3A	111.3 (2)	C1B–C2B–C3B	111.8 (2)
C2A–C3A–C4A	120.2 (2)	C2B–C3B–C4B	119.7 (2)
C2A–C3A–C8A	121.0 (2)	C2B–C3B–C8B	121.8 (2)
C4A–C3A–C8A	118.8 (2)	C4B–C3B–C8B	118.4 (2)
C3A–C4A–C5A	120.2 (3)	C3B–C4B–C5B	120.0 (2)
C4A–C5A–C6A	121.1 (3)	C4B–C5B–C6B	120.9 (3)
C5A–C6A–C7A	118.7 (2)	C5B–C6B–C7B	119.3 (3)
C6A–C7A–C8A	121.9 (3)	C6B–C7B–C8B	120.4 (3)
C3A–C8A–C7A	119.4 (2)	C3B–C8B–C7B	121.0 (2)
C1A–O1A–H1A	109 (2)	C1B–O1B–H1B	109 (2)
C2A–O3A–H3A	110 (2)	C2B–O3B–H3B	112 (2)
O3A–C2A–H2A	111 (1)	O3B–C2B–H2B	114 (1)
C1A–C2A–H2A	104 (1)	C1B–C2B–H2B	107 (1)
C3A–C2A–H2A	109 (1)	C3B–C2B–H2B	105 (1)
C3A–C4A–H4A	117 (1)	C3B–C4B–H4B	120 (1)
C5A–C4A–H4A	123 (1)	C5B–C4B–H4B	120 (1)
C4A–C5A–H5A	121 (1)	C4B–C5B–H5B	122 (1)
C6A–C5A–H5A	118 (1)	C6B–C5B–H5B	117 (1)
C5A–C6A–H6A	116 (2)	C5B–C6B–H6B	125 (2)
C7A–C6A–H6A	125 (2)	C7B–C6B–H6B	116 (2)
C6A–C7A–H7A	119 (1)	C6B–C7B–H7B	117 (2)
C8A–C7A–H7A	119 (1)	C8B–C7B–H7B	122 (2)
C3A–C8A–H8A	118 (1)	C3B–C8B–H8B	119 (1)
C7A–C8A–H8A	123 (1)	C7B–C8B–H8B	120 (1)

thermal motion of the phenyl ring which results in a significant shortening of the C(5)–C(6) and C(7)–C(8) bonds. In each molecule the C–OH group is syn to the C=O bond of the carboxyl group, with O(H)—C—C=O torsion angles of −2.2° and 1.2°, respectively. The major difference in the conformation of the two molecules is in the angle of twist of the phenyl group about the

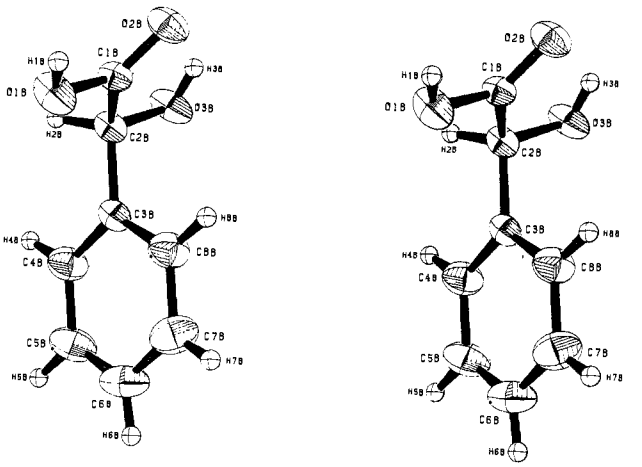

Figure 3. Stereopair drawing of molecule B, showing the numbering of the molecule. The numbering of the A molecule is analogous.

Table III. Hydrogen Bond Dimensions for (*S*)-(+)-Mandelic Acid

	molecule A	molecule B
	Intramolecular	
O(3)···O(2)	2.650 (4) Å	2.666 (4) Å
H(3)···O(2)	2.19 (3) Å	2.24 (2) Å
O(3)-H(3)···O(2)	119 (2)°	114 (2)°
	Intermolecular	
O(1)···O(3)[a]	2.632 (4) Å	2.642 (4) Å
H(1)···O(3)[a]	1.88 (2) Å	1.83 (2) Å
O(1)-H(1)···O(3)[a]	165 (3)°	162 (3)°
O(3)···O(2)[b]	2.827 (3) Å	2.848 (2) Å
H(3)···O(2)[b]	2.21 (3) Å	2.16 (3) Å
O(3)-H(3)···O(2)[b]	137 (2)°	144 (2)°

[a] The acceptor oxygen in both molecules is related by x, $1 + y$, z. [b] The acceptor oxygen in molecule A is related by $1 - x$, $-^1/_2 + y$, $1 - z$, and in molecule B by $2 - x$, $-^1/_2 + y$, $1 - z$.

C(2)–C(3) bond. In molecule A, the phenyl group is oriented so that the C(1)–C(2) bond is almost normal to the plane of the ring, i.e., the C(8)–C(3)–C(2)–C(1) torsion angle is 90.4°, whereas the corresponding angle in molecule B is 42.5°. The definite location of the carboxyl hydrogen atoms and the clear distinction in the values of the carboxyl C–O bonds and C–C–O angles argue against the presence of crystallographic disorder in the carboxyl group as is often found in substituted benzoic acids.[13]

The crystal structure is made up of chains of hydrogen-bonded mandelic acid molecules running along the *b*-crystallographic direction. Each individual chain consists of only A molecules or B molecules. Molecules translationally related along *b* in the chain are involved in intermolecular O(1)–H···O(3) hydrogen bonding. The O(3)–H hydroxyl group, in addition to being the acceptor of the hydrogen bond that forms the chain, acts as a bifurcated hydrogen bond donor, intramolecularly to the C=O(2) group and intermolecularly to a C=O group in a parallel screw-related chain;

(13) Leiserowitz, L. *Acta Crystallogr.* **1976**, *B32*, 775–801.

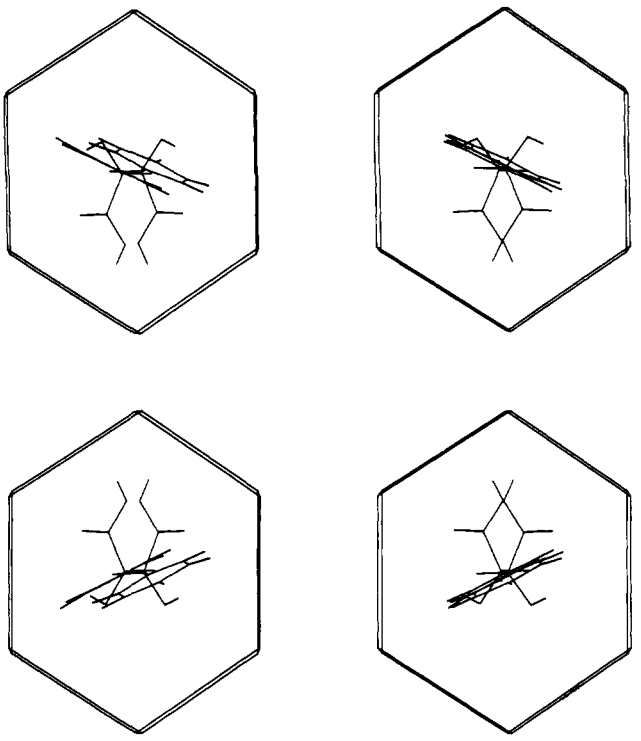

Figure 4. Sketches of crystals in the same orientation is in Figure 1 with the structures of the two molecules in the unit cell drawn in. Top drawing: (*R*)-(−)-mandelic acid. Bottom drawing: (*S*)-(+)-mandelic acid. Note that the pyroelectric effect (see Figure 1) has shown that the carboxylic OH vectors are directed toward the positive end of the crystal in each case.

thus two chains, consisting of only one type of mandelic acid molecule, are cross-linked by O-(3)-H···O(2) hydrogen bonds. The hydrogen-bonding dimensions are given in Table III. The cross-linked chain consisting only of molecules of type A is related to another cross-linked chain consisting of only B molecules by a pseudocentering in the *a* and *b* directions. There are no hydrogen-bonded contacts between such related chains. Presumably the difference in twist of the phenyl groups in the two molecules is a result of the packing interactions involved in the assembly of the structure in the *a* direction. All of the phenyl groups have the C(6)-H(6) bond pointing toward and almost perpendicular (84–85°) to the (001) or (00$\bar{1}$) faces of the crystal.

There are a number of points of similarity between the structure of (*S*)-**2** and the racemic compound whose structure was reported by other investigators.[6] The hydrogen-bonding arrangement of the (±) structure involves, as does the (*S*) structure, hydrogen bonds between the alcoholic hydroxyl groups and the carboxyl oxygens and between the carboxylic hydroxyl groups and the alcoholic oxygen atoms. However, in the case of the racemate, pairs of molecules related by centers of symmetry form hydrogen-bonded dimers which are in turn linked into a chain by further hydrogen bonds. Again the phenyl groups are almost perpendicular to the major (in this case {001}) faces.

Relationship between the Absolute Configuration of (*S*)-(+)-2 and Crystal Morphology. Since the time of Pasteur[14] it has been recognized that there may be a relationship between the development of crystal faces and the absolute configuration of the molecules in a chiral crystal. More recently Lahav, Leiserowitz, and their collaborators[15] have had much success in correlating absolute configuration with crystal growth and dissolution, including use of the development of etch pits on the crystal surfaces.[16]

Crystals of the enantiomers of mandelic acid have no faces which reveal the chirality of the crystal but, with the aid of a method of determining the absolute orientation of molecules along the polar *b* axis, the assignment can be made. In Figure 4 is shown the structure of the two independent molecules of (*S*)-(+)-**2** superimposed on a drawing of a crystal of that enantiomer together with a comparable drawing of the (*R*)-(−) isomer. Note that if the absolute molecular configuration is known the orientation of the molecules along the polar axis of a crystal can be determined from the crystal morphology. Thus, if a crystal is oriented with the *b* axis vertical in the plane of the page and with the outward-pointing (100) face to the right and the opposite inward-pointing face to the left as shown in Figure 4, the absolute configuration of the molecules determined previously by chemical means[17] shows that the O-H bonds of both the carboxyl groups and the alcoholic hydroxyl groups of each independent molecule are oriented with the oxygen→hydrogen vector toward the top of the page. Note that an additional molecule in the unit cell is produced by rotation around *b* of the parent molecule by the screw axis. Because of this, if the crystal in Figure 4 had been turned upside down by rotation 180° around *b* it would appear identical with the crystal shown with the O-H vectors still pointing toward the top of the page. In the same way a crystal of (*R*)-(−)-**2** in the same orientation [(100) up to the right] has the O-H bonds with the hydrogen atoms directed toward the bottom of the page.

Orientation of Molecules of Acid 2 along the Polar *b* Axis and ab Initio Calculation of the Molecular Dipolar Moments of the Mandelic Acid Molecule. From the discussion above it is clear that there is a direct correlation between the orientation of the mandelic acid molecules along the polar *b* axis in the crystal and the absolute configuration of the molecules in the crystal. This relationship becomes of practical value if we can predict the direction of the electric dipole moment of molecules in the orientation found in the crystal and if we can measure experimentally the direction of the electrical dipole of a particular crystal.

The symmetry of crystal class 2 has the *b* axis as the only polar crystal axis, and the only nonpolar directions are those perpendicular to *b*.[18] The angles made by the OH and COOH groups with *b* are therefore of prime interest in analyzing the relationship of molecular geometry of the two independent molecules to the crystal dipole moment. It is of particular interest that the C=O

Table IV. Ab Initio (431G/SCFO) Energies and Dipole Moments of the Two Molecules (A and B) of (*S*)-Mandelic Acid

	molecule A	molecule B
total energy (au)	−531.17728	−531.19287
μ_x (D)[a]	−1.17	1.08
μ_y (D)[a]	2.37	1.75
μ_z (D)[a]	−0.78	1.78
$\lvert\vec{\mu}\rvert$ (D)	2.75	2.72

[a] The orthogonal molecular axes used in the dipole calculation were chosen separately for the two independent molecules. The *X* and *Y* axes lie in the best plane of the phenyl ring, while the *Z* axis is normal to that plane. A matrix to convert the orthogonal crystal coordinates ($A = ax$, $B = by$, $C = cz \sin \beta$) to the dipole coordinate system for molecule A is

$$\begin{bmatrix} -0.5961 & 0.0119 & 0.3299 \\ -0.1838 & 0.9858 & -0.5491 \\ -0.6927 & 0.2001 & 0.7529 \end{bmatrix}$$

and to that for molecule B is

$$\begin{bmatrix} -0.3672 & -0.0405 & 0.6327 \\ -0.0606 & 0.9581 & -0.3859 \\ -0.7812 & 0.2203 & 0.6356 \end{bmatrix}$$

(14) Pasteur, L. *Ann. Chim. Phys.* **1850**, [3] *28*, 56–61. See ref 2a–2c for our earlier discussion of this subject.

(15) See: (a) Addadi, L.; Berkovitch-Yellin, Z.; Weissbuch, I.; van Mil, J.; Shimon, L. J. W.; Lahav, M.; Leiserowitz, L. *Angew. Chem., Int. Ed. Engl.* **1985**, 466–485 (1985). (b) Weissbuch, I.; Shimon, L. J. W.; Addadi, L.; Berkovitch-Yellin, Z.; Weinstein, S.; Lahav, M.; Leiserowitz, L. *Isr. J. Chem.* **1985**, 353–362, 362–372.

(16) Shimon, L. W. J.; Lahav, M.; Leiserowitz, L. *J. Am. Chem. Soc.* **1985**, *107*, 3375–3377.

(17) (a) Mislow, K. *J. Am. Chem. Soc.* **1951**, 3954–3957. (b) See: Eliel, E. *Stereochemistry of Carbon Compounds*; McGraw-Hill: New York, 1962; Chapter 2.

(18) Hahn, T.; Klapper, H. *International Tables for Crystallography*; The Kynoch Press: Birmingham, England, 1983, Vol. A, Table 10.5.2, p 783.

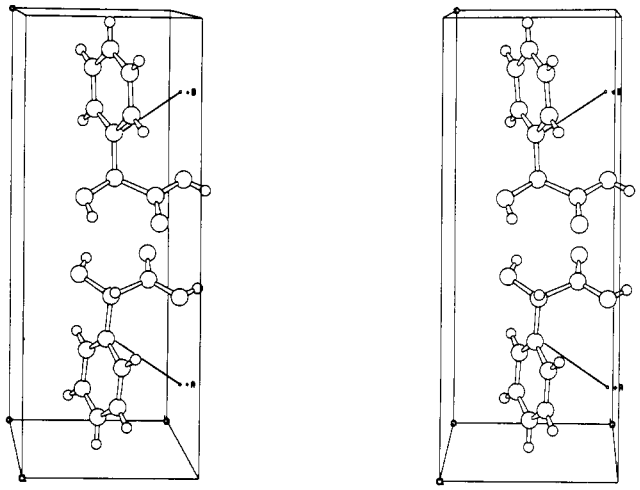

Figure 5. Stereopair drawings of the two independent molecules of (*S*)-(+)-mandelic acid in the unit cell with the magnitude and direction of the dipole represented by a line from C(3) as the negative end and with the positive end marked by A and B, respectively.

vectors in the independent molecules are almost normal to *b* (87.8 and 87.1°) and so make a negligible contribution to the crystal dipole moment. The vectors from the carbon C(1) to the hydroxyl proton H(1) of the carboxylic acid groups of each of the independent molecules in the (*S*)-(+) structure point along *b* in the positive direction making angles with *b* of 13.5 and 12.3°. Vectors from the carbon C(2) to the hydroxylic proton H(3) point also along the positive direction of *b* but make angles with *b* of 64.6° and 63.5°, respectively.

It seemed difficult to obtain a reliable estimate of the molecular dipole moment by vector addition of group moments. For this reason ab initio, self-consistent field (SCF) wave functions were computed on the two molecules (A and B) of (*S*)-(+)-mandelic acid as found in the crystal. A 431G basis set[19] totalling 115 contracted Gaussian functions was used. The dipole moments and total energies for mandelic acid are given in Table IV.

Very high level ab initio treatments can yield dipole moments accurately. However, the best of the ab initio methods would present a most challenging computational task if applied to mandelic acid. Fortunately, the dipole moments of large organic molecules tend to be most dependent on gross features of the charge distribution just because of their size, and certain of the subtle electronic structural features that are important in the dipoles of small molecules such as carbon monoxide (CO) can be ignored.

While the numerical values (2.75 and 2.72 D) for the dipole moments of the two independent molecules obtained by the 431G basis set are in good agreement, it is the orientation of the dipole moment vector with respect to the crystal axis that is of most interest. Major components in each case point along the positive direction of the polar *b* axis. These dipole calculations are on two isolated molecules in the orientation found in the crystal. They are not calculations of the dipole moment of the crystal itself and certainly do not take into account the effect of hydrogen bonding, for example. However, while the values of the calculated dipole moments should be considered only qualitatively significant the calculated orientation of the dipoles should be quite reliable. In Figure 5 is a stereopair drawing of the two independent molecules in the unit cell with the lengths and directions of the calculated dipole moments represented by a vector with origin at C(3).

A convenient experimental method for determination of the direction of the electric dipole moment of a crystal is based on a test for the absence of a center of symmetry devised by Kundt.[20,21] On the basis of the pyroelectric effect, it consists of spraying on a single crystal which had been heated or cooled a mixture of powders which develop opposite electrostatic charges when their particles separate. A particularly satisfactory choice of powders was developed by Burker[20] and consisted of lycopodium powder (dyed with methylene violet) as the positive component and flowers of sulfur and carmine which become negative. Recently we have shown that this test could be used to locate the positive ends of crystals of *p*-bromobenzoic anhydride.[5] From the absolute configuration of (*S*)-(+)-**2**, the crystal structure determination, and the direction of the molecular dipole moment just discussed, the positive end of a mandelic acid crystal can be identified as that directed toward the top of the page in Figure 4. When crystals of this configuration were subjected to the pyroelectric test[21] there was good color separation, the upper pole of the crystal attracting the sulfur and carmine with the lower pole attracting the lycopodium powder, as indicated in Figure 1. Conversely crystals of (*R*)-(−)-**2** had the colors reversed. The direction of the electric dipole of the (*S*)-(+) crystal identified by the pyroelectric test is thus in agreement with that determined from the crystal morphology, known absolute configuration, and dipole moment from the ab initio calculation. It should be emphasized that the pyroelectric test, had the absolute configuration of mandelic acid been unknown, could have been employed to determine it from the other information by reversing the argument presented here. While this result is very satisfying, before total reliance is placed on pyroelectric test results, it is desirable that there be further applications to crystals where there are independent confirmations of the absolute direction of the crystal orientations.

Reaction of (*S*)-(+)-2 with (*S*)-(−)- and (*R*)-(+)-1-Phenylethylamine. Exposure of a crystal of (*S*)-(+)-**2** to vapor of (*R*)-(+)-amine **1** showed an increase in weight corresponding to 50% reaction after 24 h. X-ray diffraction showed reflections corresponding to unreacted acid together with powder lines attributed to the (+)-(+) or, using the nomenclature of Jacques, Collet, and Wilen,[7] the p salt. After 9 days the elemental analysis was that to be expected for the 1:1 salt. The pronounced preference reported earlier[1] by amine (*S*)-**1** vapor for crystals (*R*)-**2** was confirmed. A competition experiment was carried out by placing drops of liquid (*S*)-**1** near enantiomeric crystals of the acid; both needles and "hexagonal" plates of the acid showed a preference for the chiral amine of like sign of rotation, that is the (−)(−) or the p diastereomer was formed preferentially. A careful study of the preferential crystallization of these diastereoisomeric salts from aqueous solution by Ingersoll, Babcock, and Burns[22] had shown that when (±)-mandelic acid in aqueous solution was combined with the amine in hot water the first fraction to separate was practically pure n salt. Solubility measurements by Leclercq and Jacques[23] have shown that the p salt is much more soluble

(19) Ditchfield, R.; Hehre, W. J.; Pople, J. A. *J. Chem. Phys.* **1971**, *54*, 724–728.

(20) See: (a) Lang, S. B. *Sourcebook of Pyroelectricity*; Gordon and Breach: New York, 1974. (b) Hull, H. H. *J. Appl. Phys.* **1949**, *20*, 1157–1159. (c) Buerger, M. J. *Elementary Crystallography*; Wiley: New York, revised printing 1956; pp 187–189. There seems to have been little attention to the problem of correlating the direction of the electric dipole moment with the internal crystal structure of organic crystals, however.

(21) It has long been known that electrically polar crystals, when heated, develop a positive charge at one end and a negative charge at the other but that when the same crystal is cooled below room temperature instead of being heated the polarization is reversed.[20] That end which becomes positive on heating (and negative on cooling) has been called the analogous pole and the opposite end the antilogous pole of the crystal. A number of crystal drawings in Groth's five-volume *Chemische Kristallographie*,[3] published over the years 1906–1919, have shown drawings of crystals whose morphology indicated they were non-centrosymmetric and have indicated the analogous pole in the drawing. We have found [S. Chakraborty, unpublished] that heated crystals of mandelic acid when sprayed with the powder at any point during the time of cooling to room temperature gave the same results as when the test was conducted on a heated crystal which had not been allowed to cool. Thus the (+) end of the crystal described in the present work would have been called the "analogous pole" in the older literature. It has been pointed out[20a] that a true pyroelectric effect cannot be readily separated from the piezoelectric effect. For our present purposes we shall not attempt such a distinction but will use the term "pyroelectric effect" even though there may be a substantial piezoelectric component.

(22) Ingersoll, A. W.; Babcock, S. H.; Burns, F. B. *J. Am. Chem. Soc.* **1933**, *55*, 411–416.

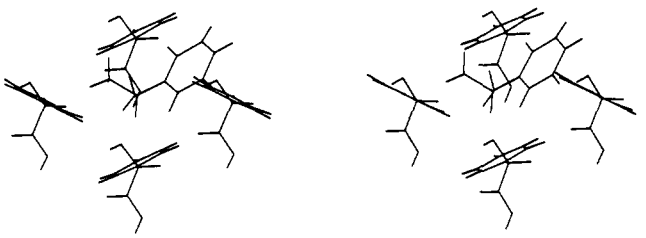

Figure 6. A portion of the major (001) face of a crystal of (*S*)-(+)-mandelic acid showing four molecules (two of A and two of B) forming a pocket through which there is possible access to the carboxyl groups. Above the four mandelic acid molecules is suspended a molecule of (*R*)-(+)-1-phenylethylamine (with coordinates derived from those in the structure of the amine salt of ref 25). The amine is shown with the $C-NH_2$ bond pointing directly into the plane of the page in an arbitrary position and orientation as an indication of the relative sizes of the molecule and the cavity in the surface.

than the n both at 10° and 30°.

Before any attempt at correlation of the preferred formation of p salt with structure can be made it is necessary to consider the direction from which the amine attacks, that is possible reaction anisotropy. Microscopic examination of "hexagonal" plates undergoing reaction shows, in the very early stages of reaction, pronounced coating of the faces cutting the polar *b* axis, $(11\bar{1})$, $(\bar{1}11)$, $(\bar{1}\bar{1}1)$, and $(1\bar{1}\bar{1})$, occurs. There is no discernable preference for attack at one end of the polar axis over the other. No extensive frontal migration develops from these faces, however, possibly because a layer of salt develops which is not easily penetrated by amine molecules. Instead reaction proceeds principally by formation of nucleation sites in the major (001) face and spread of the reaction from them. This suggests that the stereoselectivity may be due to a large extent to the relatively easy penetration of the (001) face by the amine enantiomer giving the p salt.[24,25] Although this face, as with the major faces of many benzoic acids and anhydrides, is made up of layers of phenyl rings edge on, in this case there is loose packing of the aromatic rings which leaves chiral wells between the phenyl rings through which the amine may be able to penetrate to gain access to the carboxyl groups at the bottom of the wells (see Figure 6). Such a well containing a molecule of (*R*)-(+)-amine bears a diastereomeric relationship to a well containing (*S*)-(−)-amine. Thus, the selectivity shown by one of the enantiomeric mandelic acids may be rationalized in terms of the relative fits of (+)- and (−)-amine in a well shown in Figure 6. Unfortunately, the difference in geometry of the two surfaces (made diastereoisomeric by the interaction with the chiral amine molecules) is too subtle to permit an estimate of their relative energies by inspection.

Single crystals of (*S*)-(+)-**2** exposed to ammonia vapor under conditions employed previously for reactions of other crystalline acids with ammonia melted in approximately 5 min even when the ammonia was introduced at a very slow rate. One factor may be the difficulty in reorganizing the hydrogen bonding network required for the stable form of the ammonium salt. (±)-2-Butylamine and *tert*-butylamine each reacted readily with (*S*)-(+)-**2**; *tert*-butylamine had reacted completely in 24 h. Each showed more clearly initial preferential attack at the end faces cutting the *b* axis and a greater tendency to react from the side faces of the crystal in preference to the major face (001). Crystals of (±)-**2** showed similar behavior with gaseous amines, but they reacted with less marked anisotropy than the enantiomers. A most striking observation made in the reactions of all the amines studied was that the volume expansion along the *a* and *b* axes was very small and the depth of the reacting crystal could be observed microscopically approximately to double. Just how this is related to the mechanism of the reaction remains to be explained.

Acknowledgment. This material is based on research activity supported by the National Science Foundation under Grant CHE 82-09393.

Registry No. (*S*)-**1**, 2627-86-3; (*R*)-**1**, 3886-69-9; (*R*)-**1**·(*S*)-**2**, 106336-16-7; (*S*)-**2**, 17199-29-0; (*R*)-**2**, 611-71-2; (±)-**2**, 611-72-3; ammonia, 7664-41-7; (±)-2-butylamine, 33966-50-6; *tert*-butylamine, 75-64-9.

Supplementary Material Available: Table of thermal parameters of (*S*)-mandelic acid (1 pages); listings of observed and calculated structure factors for (*S*)-mandelic acid (9 pages). Ordering information is given on any current masthead page.

(23) Leclercq, M.; Jacques, J. *Bull. Soc. Chim. Fr.* **1975**, 2052–2056.
(24) The crystal structure of the p salt has not been reported. For the structure of the n salt see: Brianso, M.-C. *Acta Crystallogr.* **1978**, *B34*, 679–680.
(25) It has been suggested by a referee that the preferential reaction to form the p salt may be due to the fact that the p salt forms a generally poor barrier to diffusion of the amine. On the basis of the data presently available, we cannot rule out this possibility.